

Action Priors for Large Action Spaces in Robotics

Anonymous Author(s)

Submission Id: 647

ABSTRACT

In robotics, it is often not possible to learn useful policies using pure model-free reinforcement learning without significant reward shaping or curriculum learning. As a consequence, many researchers rely on expert demonstrations to guide learning. However, acquiring expert demonstrations can be expensive. This paper proposes an alternative approach where the solutions of previously solved tasks are used to produce an action prior that can facilitate exploration in future tasks. The action prior is a probability distribution over actions that summarizes the set of policies found solving previous tasks. Our results indicate that this approach can be used to solve robotic manipulation problems that would otherwise be infeasible without expert demonstrations.

KEYWORDS

reinforcement learning, deep learning, action prior, robotics, robotic manipulation

ACM Reference Format:

Anonymous Author(s). 2021. Action Priors for Large Action Spaces in Robotics. In *Proc. of the 20th International Conference on Autonomous Agents and Multiagent Systems (AAMAS 2021), London, UK, May 3–7, 2021*, IFAAMAS, 12 pages.

1 INTRODUCTION

Advances in deep learning have made model-free robot control a viable alternative to model-based motion planning [5, 13, 28]. However, the complexity of tasks solvable by these approaches without extra supervision is limited, partly due to sample inefficiency of deep learning [29]. Hand-crafted temporal abstraction of end-to-end motions such as picking, placing and pushing are a compelling alternative, as they allow agents to reason over longer timescales [12, 31, 32]. In particular, Zeng et al. [32] proposed a pixel-wise parameterization of the action space, where each pixel in the observed image of the workspace corresponds to a reaching action to that position followed by a pick or place.

While both low-level action spaces with long time horizons and pixel-wise action spaces are difficult to explore, the pixel-wise parameterization makes this challenge more explicit: the agent is presented with thousands of possible actions, and usually only a handful of them enable the agent to make progress toward the goal. Exploration challenges like this are often addressed using reward shaping, curriculum learning, or imitation learning. However, these methods require additional supervision that maybe difficult to provide. Ideally, our agent could learn new skills without expert supervision.

In this paper, we construct priors over the action space – *action priors* – that inform the agent of actions that were useful in the

context of previously learned tasks. The idea of action priors has existed for some time. Sherstov and Stone [21] considered a single action prior for all states; later, this idea was extended to state-specific priors [1, 4, 18, 19]. However, to date, action priors have not been applied outside of learning in grid-world-like environments with small action spaces [4, 18, 19, 21] and planning in factored models [1].

In contrast, we train action priors in environments with image states and pixel-wise action spaces with thousands of actions. To that end, we represent an action prior as a single fully-convolutional neural network trained to summarize a library of pre-trained policies. We distinguish between a set of training tasks, which we solve using imitation learning, and a held-out set of testing tasks to be solved without expert information. The role of action priors is to bias exploration on the testing tasks toward actions that were found to be useful when solving the training tasks.

We evaluate our approach in the context of a set of 16 robotic block construction tasks. We proceed in three stages. First, our agent uses imitation learning to find near-optimal solutions to a subset of the 16 tasks. Second, we condense these near-optimal policies onto a state-dependent probability distribution over actions (i.e. the action prior) that gives high probability to any action that was part of one of the near optimal policies. Finally, we use the action prior to bias exploration when solving a new task. In the block construction domain, this action prior gives high probability to picking actions that are likely to lift a block of some type or placing actions that are likely to result in a stable placement. Although we explicitly focus on robotic manipulation, this approach should generalize well to any problem in robotics with a large action space.

This paper makes two main contributions. First, we show that a state conditioned action prior is an effective way to transfer knowledge from previously solved tasks to new tasks in a robotic manipulation domain. Our experimental results indicate that this approach can dramatically increase the probability of visiting a goal state during exploration. Second, we introduce a method of learning a state conditioned action prior in situations where the previously learned policies are valid over different regions of the state/action space. This problem only occurs in large state/action spaces such as in robotic manipulation and we believe we are the first to address it.

2 RELATED WORK

Action priors bias action selection during the exploration phase of learning towards actions that were previously determined to be viable. This information can either be specified by an expert [1] or extracted from policies from previously solved tasks [1, 4, 18, 19, 21]. Sherstov and Stone [21] eliminated actions not optimal for any previous task in a state-agnostic way. Together with their transfer learning algorithm, the state-agnostic action prior increases learning speed in grid-world mazes. Fernández-Rebollo and Veloso

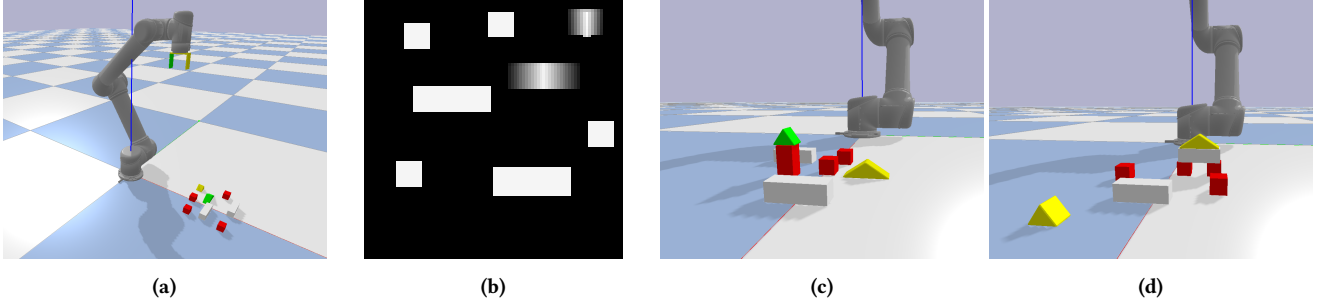


Figure 1: Our PyBullet block stacking setup. (a) a simulated UR5 arm and a 60×60 cm workspace with blocks, **(b)** a simulated top-down depth camera image of the workspace, **(c)** and **(d)** are examples of the goals states of 2 of our 16 block stacking tasks.

[4], Rosman and Ramamoorthy [18, 19] explored state-specific action priors in similar discrete-state-space MDPs. Fernández-Rebollo and Veloso [4] alternated between rolling out the policy being learned and a policy sampled from a library. The probability distribution over the library of policies was updated online to maximize rewards for the current task. Rosman and Ramamoorthy [18, 19] filled in the pseudo-counts of Dirichlet distributions used to select actions in each state by a weighted-sum of actions selected by previously learned policies. Abel et al. [1] combined action priors and hand-crafted object-oriented representations [3] to improve the run time of dynamic programming policy search for a Minecraft environment and a real-world robotic manipulation task.

In contrast to pre-defined factored representations in Abel et al. [1], we learn the action prior and model-free policies from pixels. The Dirichlet prior [18, 19] is not easily extensible to continuous state spaces; instead, we learn the action prior as a convolutional network. Compared to Fernández-Rebollo and Veloso [4], we cannot keep a library of policies loaded in memory, as each policy is parameterized by a large convolutional network—we distill all policies into a single action prior network.

The topic of **efficient exploration** is closely related to action prior. Methods in this category often do not use additional information such as prior policies. Instead, they use a notion of surprise or information content of a visited state. These quantities can be measured by counting the number of times states were visited [22] or by model-based approaches [10, 15]. Our problem statement is incomparable with these approaches, as we exploit additional information from previously learned tasks, which facilitates much more targeted exploration compared to the notion of surprise alone.

Transfer learning has been studied extensively both in classical reinforcement learning [23] and in deep reinforcement learning [7, 24]. Goyal et al. [7], Teh et al. [24] learned a so-called default policy while learning multiple specialized policies in a multi-task or a multi-goal setting. To transfer to new tasks, Teh et al. [24] used the KL-divergence between the default policy and a new policy as regularization, whereas Goyal et al. [7] used their default policy to quantify the notion of a "decision state": a state in which we need make a decision based on the task we want to solve (e.g., a crossroads in a maze). Their agent is then encouraged to explore decision states by adding an intrinsic reward.

Both Goyal et al. [7], Teh et al. [24] focuses their experimental evaluation on navigation tasks, with the latter transfer method

only being applicable to discrete-state-space domains (due to them using count-based exploration). We do not test the KL-divergence between policies [24] because we use deep Q-learning [14] instead of explicitly learning stochastic policies, but we do experiment with sharing weights between networks.

3 BACKGROUND

We model the pick and place robotics tasks in this paper as episodic Markov Decision Processes (MDPs, [2]) $\mathcal{M} = \langle S, A, P, R, \rho_0, \gamma, H \rangle$. S and A represent the sets of state and actions, $P : S \times A \times S \rightarrow [0, 1]$ is the probability of transitioning from one state to another under a selected action and $R : S \times A \rightarrow \mathbb{R}$ maps state-action pairs to their expected rewards. We consider MDPs with a finite time horizon H , an initial state distribution ρ_0 and a discount factor γ .

A policy $\pi : S \times A \rightarrow [0, 1]$ captures the decision making process of an agent as the probability distribution over actions for each state. Each policy has an associated state-action value function $Q_\pi(s, a) = R(s, a) + \gamma \mathbb{E}_{s' \sim P, a' \sim \pi} [Q_\pi(s', a')]$, the discounted return when executing action a in state s and following policy π thereafter.

In this paper, we consider MDPs with the following properties:

- States are represented as images,
- the action space is large, usually one action per state pixel,
- the time horizon is short, around 10 time steps, and
- rewards are sparse.

Learning an optimal policy for this class of MDPs without additional information is extremely difficult because there is only a handful of optimal actions in each state. Hence, the probability of getting a reward for a sequence of random actions is minuscule.

4 PROBLEM STATEMENT

Let $T_{\text{train}} = \{T_1, T_2, \dots, T_N\}$ be a set of training tasks expressed as MDPs. A task $T_i = \langle S, A, P_i, R_i, \rho_0, \gamma, H \rangle$ shares its definition with all other tasks except for its reward and transition function. For example, a task of building a tower from blocks of height two and a task of building a tower of height three clearly have a different reward function. Even though the dynamics of picking and placing objects are the same for both tasks, the former task terminates when a tower of two is built, whereas the latter does not. Therefore, there are small variations in the transition function between the tasks related to terminal states.

Algorithm 1 Action prior learning

Input: Set of training tasks $T = \{T_1, T_2, \dots, T_N\}$.
Output: Action prior network f_{AP} .

```

1: procedure LEARNAP
2:   for  $T_i$  in  $T$  do
3:     Use expert demonstrations to train  $\pi_i$  (Section 5.1)
4:     Collect  $K$  transitions by rolling out  $\pi_i$ . Store states visited in  $D_i$ 
5:   end for
6:   Concatenate datasets  $\{D_1, D_2, \dots, D_N\}$  into  $D$ 
7:   Train task classifier  $f_C : S \rightarrow \Delta^{N-1}$  on  $D$  (Section 5.2)
8:   Collect optimal action sets for  $\pi_1, \dots, \pi_N$  on  $D$ 
9:   Merge optimal action sets using  $f_C$  and add the union set to  $D$  (Section 5.3)
10:  Train action prior network  $f_{AP} : S \times A \rightarrow [0, 1]$  on  $D$ 
11:  Return  $f_{AP}$ 
12: end procedure
```

We assume we have access to a near-optimal policy π_i for each task i together with a dataset of on-policy transitions D_i and an approximate state-action value function Q_{π_i} . Given a new task T_{N+1} that differs in its transition and reward dynamics from the training task, our goal is to learn the best possible policy π_θ given the experience of learning the previous task

$$\arg \max_{\theta} \mathbb{E}_{\pi_\theta, \rho_0, P_{N+1}} \left[\sum_{t=0}^H \gamma^t R_{N+1}(s_t, a_t) \middle| (D_i, \pi_i, Q_{\pi_i})_{i=1}^N \right]. \quad (1)$$

5 METHODS

Given a set of near-optimal policies π_1, \dots, π_N for tasks $T_i \in T_{\text{train}}$, we define the action prior to be a policy

$$\pi_{AP}(s, a) = \eta \max_{i \in [1 \dots N]} \pi_i(s, a),$$

where η is normalizes π_{AP} . For example, if π_1, \dots, π_N are deterministic, then π_{AP} assigns equal probability to each action $\pi_1(s) \dots \pi_N(s)$.

Algorithm 1 outlines the procedure we use to train the action prior. First, we find near-optimal policies for the N training tasks. Step 3 accomplishes this using imitation learning (we use SDQfD [26], a variant of DQfD [9]). Then in Step 4, for each task i and policy π_i , we obtain a sample of on-policy states by rolling out π_i .

Next, in Step 7, we train a classifier f_C that predicts the task that is most likely to have caused the agent to visit a state. This is important because the policies π_i are not all valid over the entire state space. For example, a policy trained to assemble the structure in Figure 1a (tower from two cubes and a small roof) has never seen the state shown in Figure 1b (a house built from two blocks, a brick and a large roof). To determine the set of policies applicable in a given state, we train a task classifier $f_C : S \rightarrow \Delta^{N-1}$ (Section 5.2), which predicts the tasks in which a state is most frequently encountered. This allows the action prior to ignore policies for tasks that are not relevant to a particular state.

Then, in Step 8 of Algorithm 1, after training the policies π_i and the task classifier f_C , we collect the training dataset for the action prior (Section 5.3). This dataset contains an equal number of states for each task, which are obtained by rolling out the learned

Algorithm 2 Action prior exploration

Input: Deep Q-network f_{DQN} , action prior network f_{AP} , action prior probability threshold σ , task T .

```

1: procedure EXPLOREAP
2:   while Stopping condition not reached do
3:     Get environment state  $s$ 
4:     Decide if explore or exploit
5:     if explore then
6:        $\tilde{A}^* \leftarrow \{a \mid a \in A \wedge f_{AP}(s, a) > \sigma\}$ 
7:       Randomly sample  $a \sim \text{Uniform}(\tilde{A}^*)$ 
8:     else
9:        $a \leftarrow \arg \max_{a \in A} f_{DQN}(s)$ 
10:    end if
11:    Execute action  $a$  in the environment
12:    Observe reward  $r$  and next state  $s'$ 
13:    Add tuple  $(s, a, r, s')$  into the replay buffer
14:    Perform deep Q-network training step
15:   end while
16: end procedure
```

policies π_i . For each state, we compute a binary mask that represents the union of actions that are optimal (in any task) given a set of policies. The set of applicable policies is predicted by the task classifier. Step 10 of Algorithm 1 trains the action prior network $f_{AP} : S \times A \rightarrow [0, 1]$ to predict the probability of an action being optimal for any task in a given state (Section 5.4). Finally, we create an action prior policy $\pi_{AP}(s, a)$ based on the action prior network f_{AP} . By thresholding the probabilities predicted by f_{AP} , we get a set of proposed actions $A^*(s)$ for state s . We set $\pi_{AP}(s, a)$ to be a uniform distribution over $A^*(s)$ with actions outside of the optimal set being assigned zero probability.

5.1 Learning Initial Policies

We use SDQfD [26], an imitation learning algorithm similar to DQfD [9], to learn near-optimal policies π_i for the training tasks. The objective is comprised of a temporal-difference loss L_{TD} (as in DQN [14]) and a term L_{SLM} (with weight ω) that penalizes non-expert actions with high values

$$L_{SDQfD} = L_{TD} + \omega L_{SLM}. \quad (2)$$

During training, the method identifies the set of non-expert actions A_{s,a_e} with values higher than the value of an expert action a_e minus a margin $l(a_e, a)$ (positive constant for $a_e \neq a$; zero otherwise)

$$A_{s,a_e} = \{a \in A \mid Q(s, a) > Q(s, a_e) - l(a_e, a)\}. \quad (3)$$

The penalty called a "strict large margin" is then applied to the values of all actions in A_{s,a_e}

$$L_{SLM} = \frac{1}{|A_{s,a_e}|} \sum_{a \in A_{s,a_e}} Q(s, a) + l(a_e, a) - Q(s, a_e). \quad (4)$$

We pre-train SDQfD on a dataset that only contains expert demonstrations for the first T_E gradient descent steps. To avoid programming expert policies, we instead implement a planner that deconstructs a goal block structure—initializing goal states in simulation is relatively simple. A dataset of reversed deconstruction experience can be used in place of expert trajectories [30]. After pre-training,

we alternate between taking one environment step according to the current policy and performing a training step. We maintain two separate buffers: one for expert and one for on-policy transitions. Each batch of training data contains an equal number of samples from both buffers. The strict large margin is only computed for the expert data.

5.2 Learning the Task Classifier

The task classifier $f_C : S \rightarrow \Delta^{N-1}$ determines which of the initial policies are relevant in the context of a particular state. To train this classifier, we use a dataset of states and categorical labels $\{(s_i, y_i)\}_{i=1}^M$. We construct this dataset by generating policy rollouts for each task. If a state s was visited during a rollout of a policy for a task $y \in \{1, \dots, N\}$ we include the pair (s, y) in the dataset. Note that this results in a dataset where class labels for each state are not unique, as each state could have been encountered during rollouts for multiple tasks (e.g. the initial state with all objects placed on the ground appears in all tasks). We can interpret the data as samples $s_i, y_i \sim p(s, y)$ from a distribution $p(s, y) = p(s|y)p(y)$ in which $p(y)$ is a uniform prior over tasks (i.e. the training dataset is balanced), and $p(s|y)$ is the fraction of rollouts for each task in which state s appears. The classifier now approximates the conditional distribution $p(y|s) \propto p(s, y) \propto p(s|y)$.

We implement f_C as a neural network $NN(s)$ that predicts logits for all classes, which we normalize using a softmax function

$$p(y|s) \approx f_C(s) = \text{softmax}(NN(s)), \quad (5)$$

and train the classifier using a cross-entropy loss

$$L_C = -\frac{1}{M} \sum_{i=1}^M \sum_{j=1}^{|T|} \mathbb{I}[y_i = j] \log f_C(s)_j. \quad (6)$$

To determine if policy for task j is applicable in state s , we check if the predicted probability $f_C(s)_j$ is above some threshold δ .

Since neural classifiers in general do not have well-calibrated probabilities, our approximation of $p(y|s)$ can in practice be overconfident [8]. That said, we find that this classification strategy works sufficiently well for our purposes in practice.

5.3 Approximating Optimal Action Sets

For an ideal action prior, we would like to determine the set of actions $A^*(s)$ that are optimal for *any* task in state s . If we use Q_{π_i} to denote the state-action values for task i that we learned using SDQfD, then we can define the optimal action set for state s as

$$A^*(s) = \bigcup_{i=1}^N \left\{ a \mid Q_{\pi_i}(s, a) = \max_{a' \in A} Q_{\pi_i}(s, a') \right\}. \quad (7)$$

We expect the cardinality of $A^*(s)$ to be high in our domain, as there are many equivalent ways of picking and placing objects. Since the state-action values learned by SDQfD tend to be noisy, it is however non-trivial to determine the set of optimal actions without carefully setting a threshold for each trained model.

Instead, we restrict the optimal actions set to one action per task with the optimal action for the i th task denoted by a_i^*

$$\tilde{A}^*(s) = \{a_1^*, a_2^*, \dots, a_N^*\}. \quad (8)$$

These approximate optimal action sets $\tilde{A}^*(s)$ are clearly subsets of the ground-truth sets $A^*(s)$. We deal with the problem of increasing the number of proposed optimal actions in Section 5.4. Furthermore, we restrict the optimal actions set to only the task determined to be applicable by the task classifier (Section 5.2).

5.4 Learning the Action Prior

We use the approximate optimal action sets $\tilde{A}^*(s)$ to learn an action prior $f_{AP} : S \times A \rightarrow [0, 1]$, which takes the form of a multi-task classifier that returns binary predictions for all actions A given a state $s \in S$. We train this classifier using pairs of states and optimal actions masks $\{(s_i, m_i)\}_{i=1}^L$. We collect training states by rolling out the learned policies for each task for a fixed number of time steps. For each state, we then compute the optimal mask, which for each action a contains a bit that indicates whether this action is part of the approximate optimal action set

$$m_{i,a} = \mathbb{I}\left[a \in \tilde{A}^*(s_i)\right]. \quad (9)$$

We train this multi-task classifier using a standard logistic loss

$$L_{AP} = -\frac{1}{L} \sum_{i=1}^L \sum_{j=1}^{|A|} m_{ij} \log f_{AP}(s_i, a_j) + (1 - m_{ij}) \log (1 - f_{AP}(s_i, a_j)). \quad (10)$$

As discussed above, the training masks contain only a subset of the union of optimal action sets for all tasks. We can view this problem from the perspective of precision-recall trade-off. A model that achieves a low L_{AP} value will have a high precision (i.e., it will avoid false positive optimal actions), but it might have low recall because not every optimal action is represented in the training data.

This trade-off can be controlled by moving the decision boundary $\mathbb{I}[f_{AP}(s, a) \geq \sigma]$ that determines if an action is deemed optimal. Experimentally, we found that setting σ to a low value (i.e., increasing recall and decreasing precision) results in a large increase in the success rate of the action prior exploration policy.

5.5 Action prior exploration

Algorithm 2 summarizes how we use the action prior for exploration when training a deep Q-network on a new task. We follow the standard recipe of alternating between selecting random actions (exploration) and action according to the policy being learned (exploitation). The most common and one of the simplest approaches to controlling this trade-off is an ϵ -greedy exploration policy with the value of ϵ decaying over time (e.g., this approach was used in the original deep Q-network paper [14]).

We use an ϵ -greedy strategy in which, during exploration, we select actions uniformly at random from the set actions for which the action prior exceeds a threshold σ

$$\bar{A}^*(s) = \{a \mid a \in A \wedge f_{AP}(s, a) > \sigma\}. \quad (11)$$

This results in a more focused exploration compared to selecting actions uniformly at random from the full set A .

It is possible that a new task will require the agent to select an action that was not optimal in any previous tasks. In this context, it could be beneficial to occasionally select a completely random action during the exploration step. But, we find it to decrease the

Num. fruits	DQN RS		DQN AP	
	Mid.	Fin.	Mid.	Fin.
Fruit combinations				
1	100%	100%	100%	100%
2	100%	100%	100%	100%
3	99%	100%	100%	100%
4	12%	91%	100%	100%
Fruit sequences				
1	100%	100%	100%	100%
2	100%	100%	100%	100%
3	59%	97%	93%	100%
4	0%	0%	77%	97%

Table 1: Transfer learning results on the Fruit World task. There are five distinct fruits in the environment and the agent should pick up between one and four of them (Num. fruits). Picking can be done either in any order (Fruit combinations) or in a particular order (Fruit sequences). We use all possible tasks for fruit combinations (30 tasks) and sample 20 tasks for fruit sequences out of 205 possible tasks. The results were obtained by leave-one-out cross-validation, where we learn an action prior over $N - 1$ tasks and perform transfer learning on the N th task. We report success rate for a no-transfer DQN baseline (DQN RS) and a DQN with an action prior (DQN AP). The results are the success rate with zero exploration evaluated in the middle of training (Mid.) and at the end of training (Fin.). Each experiment was repeated 10 times, averages are reported.

success rate of the action prior exploration policy. We hypothesize that by setting σ to a low value (around 0.1) the action prior generalizes to actions that were not necessarily optimal for any previous task but are nevertheless plausible.

6 EXPERIMENTS

We demonstrate the effectiveness of action priors in two domains: a proof-of-concept Fruits World (Section 6.2) and a block stacking robotic manipulation experiment in the PyBullet physics simulator (Section 6.3). Policies learned in PyBullet can be deployed on a real-world UR5 robotic arm (Section 6.4). The key question we aim to answer is if action prior enables a deep Q-network to learn tasks that were previously out of reach.

Although our source code was not ready for release by the paper deadline, we commit to publishing it with the camera-ready version of our paper. We will exclude the real-world experiments, as we have hard-coded parameters specific to our physical setup.

6.1 Domains

Fruits World is a grid-world-like non-visual domain. The world is a 5×5 grid with five distinct fruits placed in random positions (the positions change at the start of each episode). There are 25 actions, one for each position. The agent must pick a subset of fruits either in a particular order (sequences) or in any order (combinations); each

subset constitutes a different task. When the agent thinks it finished the task, it must execute the 25th action to get a reward and reset the environment. A reward of 1 is given for successfully picking up the target fruits. Due to its combinatorial nature, this environment is surprisingly difficult to solve with model-free deep reinforcement learning. Hence, we also give the agent a reward of -0.1 for picking up the wrong fruit and only allow it to put the right fruits in the basket.

The observation is a $5 \times 5 \times 5$ tensor with the first two dimensions corresponding to the grid. If a fruit is present in a grid cell, its ID is one-hot encoded in the third dimension. Otherwise, the values in the grid cell are all zero.

In the combination version, a sixth channel is added to the observation: the positions corresponding to fruits the agent has added to its basket are set to one. In the sequence version, the agent is given an additional sequence of one-hot encoded IDs of fruits it has picked.

Both the DQN and the action prior models use a multilayer perceptron with two hidden layers. Please refer to Section B.1 in the Appendix for the full description of hyper-parameters.

PyBullet block stacking is a set of simulated tasks involving stacking blocks of various shapes and sizes with a robotic arm (Figure 1). The robot observes the workspace with a depth camera from above (Figure 1 (b)), receiving a 90×90 image with pixel values corresponding to heights. It can execute a top-down pick or place action at a specified coordinate with fixed hand rotation. Before executing a pick action, the robot will take a 24×24 picture centered at the coordinates, where it is executing the pick action. If it successfully picks up an object, it uses the in-hand image to decide where to place it.

We discretize the action space as a 90×90 grid, each cell corresponding to one pixel of the observation. We instantiate 16 different block stacking tasks: each one builds a structure of a width of one or two small blocks and a height of two or three blocks; each structure has a roof on top. Figure 1 (c) and (d) show goal states of building a tower from two small blocks and a small roof and of building a structure from two small blocks followed by one long block and a large roof respectively. Each task is represented as a string (e.g. a small roof on top of a small block is "1b1r") and we use a context-free grammar to generate all possible tasks with particular parameters (Appendix Section A).

Both the 90×90 observation and the 24×24 in-hand image are encoded using a modified version of U-Net [17, 26]. We chose this model because it can produce detailed segmentation maps. The task our DQNs and action prior models solve is comparable to image segmentation: we make a prediction for each pixel of the input image. In the DQN case, the U-Net predicts a single state-action value for each pixel of the input image. In the action prior case, the model produces a logit for each pixel of the observation. The exact architecture of our U-Net is depicted in Figure 6 in the appendix.

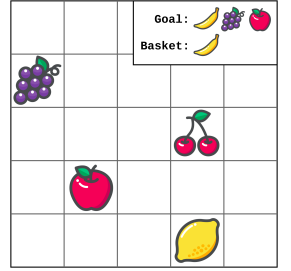


Figure 2: Sequential fruit picking task.

Method	Final success rate on task							
	1b1r	2b1r	2b2r	1l1r	1l2r	1b1b1r	2b1b1r	2b2b1r
DQN RS	100%	0%	0%	100%	100%	0%	0%	0%
DQN RS, WS	98%	0%	0%	99%	100%	0%	0%	0%
DQN HS	97%	0%	0%	100%	100%	0%	0%	0%
DQN HS, WS	97%	0%	2%	100%	99%	3%	0%	0%
DQN AP	100%	100%	98%	99%	100%	100%	93%	0%
DQN AP, WS	100%	96%	97%	99%	99%	99%	92%	0%
DQN RS	0%	0%	0%	0%	0%	0%	0%	0%
DQN RS, WS	0%	0%	0%	0%	0%	0%	0%	0%
DQN HS	0%	0%	0%	10%	0%	0%	5%	92%
DQN HS, WS	0%	0%	0%	3%	0%	0%	3%	96%
DQN AP	95%	96%	0%	100%	99%	90%	93%	97%
DQN AP, WS	0%	97%	0%	100%	100%	98%	100%	99%

Table 2: Transfer experiments in the block stacking domain. We consider "DQN AP, WS" the main contribution of this paper. Each column reports the final success rate averaged over 100 episodes after training; see Figure X for examples of the goal states for each task. The baselines and ablations of our method we consider are random action selection (RS), heuristic action selection (HS), weight sharing (WS) and action prior (AP).

6.2 Fruits world experiments

We sample 20 and 30 tasks for the fruits sequences and combinations tasks respectively (see Section 6.1 for details). Action priors are tested in a leave-one-out transfer experiment: an action prior is trained on 19 and 29 tasks respectively, and we then use it to learn the last task. This process is repeated for each task.

To learn initial policies, we first pre-train on expert demonstrations collected with an ϵ -greedy policy. That is, we either sample an optimal action or a random action. We then fine-tune the policies online, which we use to collect training data for the action prior.

We compare action priors (DQN AP) with random exploration (DQN RS) in Table 1. We divide tasks based on their complexity (the number of fruits to pick up) and average the results for each class. DQNs with action priors can learn close to optimal policy for all task difficulties, whereas random exploration fails on the most difficult sequential fruit picking tasks (last row of Table 1). Moreover, the action prior DQNs learn faster, as indicated by the performance at the midpoint of training (Mid.).

6.3 PyBullet block stacking experiments

We perform two experiments in this domain: one focused on model-free learning with action priors and the other solely on exploration using action priors. The first experiment matches the setup in Section 6.2: we use 15 out of the 16 block stacking tasks to learn an action prior, which we subsequently test on the 16th task (Table 2).

The second experiment evaluates the success rate of action prior policies on all tasks without additional training (Figure 4 shows two example tasks, Figure 8 contains the results for all tasks). We measure success rate as a function of the action prior probability threshold σ and the presence or absence of a task classifier.

Experiment #1 compares our method with two baselines. **DQN AP** is a deep Q-network with action prior exploration. We test random action selection and heuristic action selection. As our observations are depth images taken from the top of the workspace, the heuristic only allows selecting actions that act on parts of the observation with non-zero height. Therefore, it forces the agent to interact with objects. But, not all interactions necessarily lead to desirable outcomes—the agent often ends up pushing objects out of the workspace. We call the two methods **DQN RS** and **DQN HS** respectively.

As a second mechanism for speeding up learning, we employ weight sharing in the unseen task. Because an action prior summarizes the information contained in SDQfDs for the 15 training tasks, we initialize the DQN for the 16th testing task with the action prior weights. To mitigate catastrophic forgetting [6], we include a L^2 penalty between the original action prior weights and the current DQN weight; it is added to the DQN loss function with a weight of ω_{WS} . We test weight sharing both with random and heuristic baselines (**DQN RS, WS** and **DQN HS, WS**) and action priors (**DQN AP, WS**).

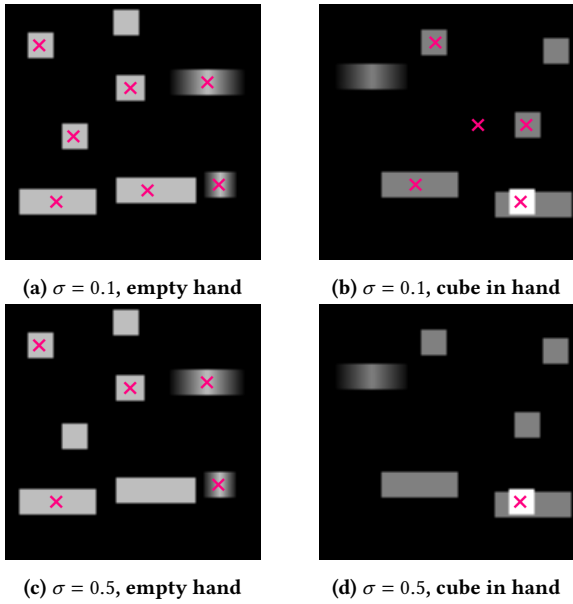


Figure 3: Visualizing actions proposed by an action prior (red crosses) with the probability threshold σ set to 0.1 (top row) and 0.5 (bottom row). In the first column, the robot is supposed to pick up an object, in the second column, it is holding a cube in its hand and wants to place it. The images shown are pictures from a depth camera mounted at the top of the workspace in simulation.

A DQN with an action prior can solve all tasks except for "2b2b1r" and "2b1l2r" (Table 2). As shown in Figure 8, the success rates of action priors on these tasks without training is between 1 and 4%. Hence, a more targeted action prior might be needed to solve these tasks.

The DQN sharing weights with the action prior does not lead to noticeable benefits. In fact, it fails to learn "2b2b2r", which the non-weight-sharing variant can solve. Since the purpose of weight sharing is mostly to improve training speed of the network, it only provides minor benefits due to exploration being the main challenge in our domains.

As we expected, both the heuristic and random action selection baselines are unable to solve most of the tasks. Random actions succeed on the three simplest tasks ("1b1r", "2b1r" and "2b2r"), and heuristic selection increases the number to four (plus "1l1l2r"). In the rest of the tasks, the success rates of the baseline exploration policies are close to zero; therefore, no learning method including weight sharing can succeed.

Experiment #2 evaluates two variants of action prior each again trained in leave-one-out fashion on 15 tasks and tested on the 16th task. In this experiment, we only log the success rate of the action prior policy without learning on the testing task.

Figure 4 shows examples of action prior success rates for tasks "1b1r" and "2b1l1r". We plot the success rates as a function of the action prediction threshold σ and the presence or absence of a task classifier. The success rates are measured by rolling out episodes in the test task (depicted in the top-left corner) with actions selected

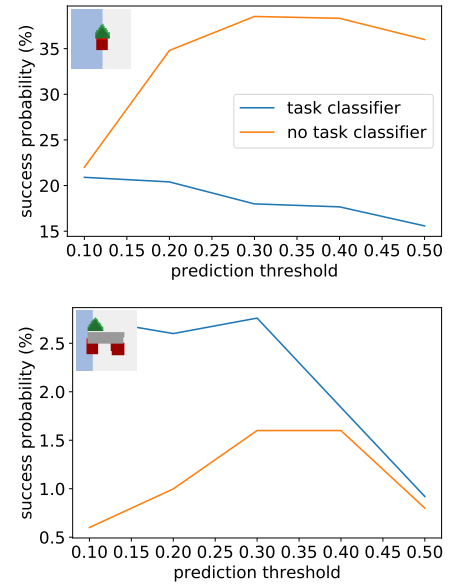


Figure 4: Success rates for "1b1r" and "2b1l1r" using exploration with an action prior as a function of σ . We compare action priors trained with and without task classifier.

by the action prior policy π_{AP} . We show results for all tasks in Appendix Figure 8.

The main trends in Figure 4 (and the Appendix Figure 8) are that (a) more complicated tasks benefit more from the action classifier and that (b) almost all action priors that use a task classifier benefit from a decrease in the prediction probability threshold. The increase in success rates for action priors with task classifiers in more complex tasks can be explained by them needing a targeted and precise exploration policy: a task classifier ensures that the training data for the action prior does not mark actions from irrelevant tasks as optimal. On the other hand, we are unsure as to why action priors without task classifiers perform well on simple tasks.

6.4 Real-world robot experiments

In theory, policies trained in our PyBullet simulation can be transferred to a real-world robot, as both setups use a depth camera and a robotic arm with the same action spaces. However, in practice noise in the real-world observations often confuses the policies trained with perfect depth images.

To make our models more robust, we re-train the action prior DQNs with weight sharing (DQN AP, WS) in the transfer learning experiment in Section 6.3 with two modifications to the environment. First, we add Perlin noise, a type of correlated gradient noise, to the simulated depth images [11, 16]. The noise models blobs of lower and higher estimated depth values that are present in the real-world images. Next, we initialize all objects in the environment with small rotations compared to their default orientations. In our previous experiments, all objects had the same orientation, as the agent cannot control the rotation of the robot hand. However, the initialization of the real-world scene will inevitably be less precise.

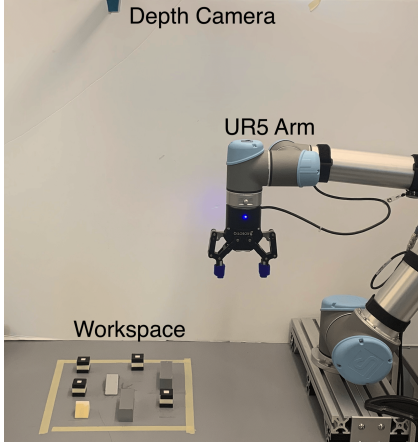


Figure 5: Our pick and place experiment with a UR5 robotic arm. The robot observes the workspace with a depth camera mounted above it, and it can choose to either pick or place an object with a top grasp and fixed orientation.

Task	Successes	# Pick Failures	# Place Failures
1b1r	9/10	1	0
1l1r	8/10	2	0
1l2r	9/10	1	0
1b1b1r	9/10	1	0
1l1b1r	10/10	0	0
1l2b2r	8/10	1	1
1l1l1r	7/10	1	2
1l1l2r	8/10	0	2

Table 3: Real-world experiment with a UR5 robotic arm (Figure 5). The environment was set up in the same way as the simulated workspace and we evaluated policies trained in simulation in 10 trials. Each trial had a budget of 20 time steps. We break down failures into two components: pick failures and place failures. Pick failures mean that the robot could not find the desired object or it could not pick it with sufficient precision. Place failures occur when the robot fails to place an object on the appropriate structure or it topples the structure over.

Our setup is depicted in Figure 5 and described in details in Appendix Section B.3. We pick 8 of the 16 trained policies for testing. Each such policy is run for ten episodes and we report the fraction of successful episodes (Table 3). Most policies reach around 80% – 90% success rate. Two common failure modes are the robot failing to find the small roof because of noise in the depth image and the robot accidentally toppling a structure over during the place action. The latter cannot always be attributed to a bad policy—our gripper sometimes releases objects off-center. Since the real-world gripper is significantly larger than the simulated one, it sometimes cannot complete the task if objects get pushed too close to each other.

7 DISCUSSION AND CONCLUSION

In this work, we proposed a method for efficient exploration using action priors. Our approach to learning action priors involves solving a set of initial tasks with imitation learning and summarizing the learned policies in a single action prior neural network. This network is trained on sets of optimal actions predicted by the policies with an addition of a task classifier that determines which policies are relevant to a particular state.

In contrast to prior work on action priors, which has predominantly considered grid-world-like environments, our method is applicable to domains with image states and thousands of actions. In addition to a proof-of-concept Fruits World domain, where it always finds near-optimal policies, we demonstrate performance on a simulated robotic block stacking task. A deep Q-network augmented with an action prior can solve 14 out of the 16 block stacking tasks within 100k episodes. Moreover, the policies trained in simulation can also be deployed on the real robotic arm with only a small drop in their success rates.

A future direction of our work is to develop action priors that are suitable to learning online during training on a new task. In this way, the action prior would progressively increase the chance of hitting the goal state while exploring. We also aim to solve tasks with even larger action spaces. A natural extension of our manipulation task is to consider rotations of the hand ($SE(2)$ space) in the top-down view or let the hand grasp the objects from different angles ($SE(3)$ action spaces).

REFERENCES

- [1] David Abel, D. Ellis Hershkowitz, Gabriel Barth-Maron, Stephen Brawner, Kevin O’Farrell, James MacGlashan, and Stefanie Tellex. 2015. Goal-Based Action Priors. In *Proceedings of the Twenty-Fifth International Conference on Automated Planning and Scheduling, ICAPS 2015, Jerusalem, Israel, June 7-11, 2015*. 306–314.
- [2] Richard Bellman. 1957. A Markovian Decision Process. *Journal of Mathematics and Mechanics* 6, 5 (1957), 679–684.
- [3] Carlos Diuk, Andre Cohen, and Michael L. Littman. 2008. An object-oriented representation for efficient reinforcement learning. In *Machine Learning, Proceedings of the Twenty-Fifth International Conference (ICML 2008), Helsinki, Finland, June 5-9, 2008*. 240–247.
- [4] Fernando Fernández-Rebolledo and Manuela M. Veloso. 2006. Probabilistic policy reuse in a reinforcement learning agent. In *5th International Joint Conference on Autonomous Agents and Multiagent Systems (AAMAS 2006), Hakodate, Japan, May 8-12, 2006*. 720–727.
- [5] Chelsea Finn and Sergey Levine. 2017. Deep visual foresight for planning robot motion. In *2017 IEEE International Conference on Robotics and Automation, ICRA 2017, Singapore, Singapore, May 29 - June 3, 2017*. 2786–2793.
- [6] Robert M. French. 1999. Catastrophic forgetting in connectionist networks. *Trends in Cognitive Sciences* 3, 4 (1999), 128 – 135.
- [7] Anirudh Goyal, Riashat Islam, Daniel Strouse, Zafarali Ahmed, Hugo Larochelle, Matthew Botvinick, Yoshua Bengio, and Sergey Levine. 2019. InfoBot: Transfer and Exploration via the Information Bottleneck. In *7th International Conference on Learning Representations, ICLR 2019, New Orleans, LA, USA, May 6-9, 2019*.
- [8] Chuan Guo, Geoff Pleiss, Yu Sun, and Kilian Q. Weinberger. 2017. On Calibration of Modern Neural Networks. In *Proceedings of the 34th International Conference on Machine Learning, ICML 2017, Sydney, NSW, Australia, 6-11 August 2017*. 1321–1330.
- [9] Todd Hester, Matej Vecerík, Olivier Pietquin, Marc Lanctot, Tom Schaul, Bilal Piot, Dan Horgan, John Quan, Andrew Sendonaris, Ian Osband, Gabriel Dulac-Arnold, John P. Agapiou, Joel Z. Leibo, and Audrunas Gruslys. 2018. Deep Q-learning From Demonstrations. In *Proceedings of the Thirty-Second AAAI Conference on Artificial Intelligence, (AAAI-18), the 30th innovative Applications of Artificial Intelligence (IAAI-18), and the 8th AAAI Symposium on Educational Advances in Artificial Intelligence (EAAI-18), New Orleans, Louisiana, USA, February 2-7, 2018*. 3223–3230.
- [10] Rein Houthooft, Xi Chen, Yan Duan, John Schulman, Filip De Turck, and Pieter Abbeel. 2016. VIME: Variational Information Maximizing Exploration. In *Advances in Neural Information Processing Systems 29: Annual Conference on Neural*

- Information Processing Systems 2016, December 5-10, 2016, Barcelona, Spain.* 1109–1117.
- [11] Stephen James, Andrew J. Davison, and Edward Johns. 2017. Transferring End-to-End Visuomotor Control from Simulation to Real World for a Multi-Stage Task. In *1st Annual Conference on Robot Learning, CoRL 2017, Mountain View, California, USA, November 13-15, 2017, Proceedings*. 334–343.
- [12] Robert Platt Jr., Colin Kohler, and Marcus Gualtieri. 2019. Deictic Image Mapping: An Abstraction for Learning Pose Invariant Manipulation Policies. In *The Thirty-Third AAAI Conference on Artificial Intelligence, AAAI 2019, The Thirty-First Innovative Applications of Artificial Intelligence Conference, IAAI 2019, The Ninth AAAI Symposium on Educational Advances in Artificial Intelligence, EAAI 2019, Honolulu, Hawaii, USA, January 27 - February 1, 2019*. 8042–8049.
- [13] Sergey Levine, Peter Pastor, Alex Krizhevsky, Julian Ibarz, and Deirdre Quillen. 2018. Learning hand-eye coordination for robotic grasping with deep learning and large-scale data collection. *Int. J. Robotics Res.* 37, 4-5 (2018), 421–436.
- [14] Volodymyr Mnih, Koray Kavukcuoglu, David Silver, Andrei A. Rusu, Joel Veness, Marc G. Bellemare, Alex Graves, Martin A. Riedmiller, Andreas Fidjeland, Georg Ostrovski, Stig Petersen, Charles Beattie, Amir Sadik, Ioannis Antonoglou, Helen King, Dharshan Kumaran, Daan Wierstra, Shane Legg, and Demis Hassabis. 2015. Human-level control through deep reinforcement learning. *Nat.* 518, 7540 (2015), 529–533.
- [15] Deepak Pathak, Pulkit Agrawal, Alexei A. Efros, and Trevor Darrell. 2017. Curiosity-driven Exploration by Self-supervised Prediction. In *Proceedings of the 34th International Conference on Machine Learning, ICML 2017, Sydney, NSW, Australia, 6-11 August 2017*. 2778–2787.
- [16] Ken Perlin. 1985. An image synthesizer. In *Proceedings of the 12th Annual Conference on Computer Graphics and Interactive Techniques, SIGGRAPH 1985, San Francisco, California, USA, July 22-26, 1985*. 287–296.
- [17] Olaf Ronneberger, Philipp Fischer, and Thomas Brox. 2015. U-Net: Convolutional Networks for Biomedical Image Segmentation. In *Medical Image Computing and Computer-Assisted Intervention - MICCAI 2015 - 18th International Conference Munich, Germany, October 5 - 9, 2015, Proceedings, Part III*. 234–241. https://doi.org/10.1007/978-3-319-24574-4_28
- [18] Benjamin Rosman and Subramanian Ramamoorthy. 2012. What good are actions? Accelerating learning using learned action priors. In *2012 IEEE International Conference on Development and Learning and Epigenetic Robotics, ICDL-EPIROB 2012, San Diego, CA, USA, November 7-9, 2012*. 1–6.
- [19] Benjamin Rosman and Subramanian Ramamoorthy. 2015. Action Priors for Learning Domain Invariances. *IEEE Trans. Auton. Ment. Dev.* 7, 2 (2015), 107–118.
- [20] Tom Schaul, John Quan, Ioannis Antonoglou, and David Silver. 2016. Prioritized Experience Replay. In *4th International Conference on Learning Representations, ICLR 2016, San Juan, Puerto Rico, May 2-4, 2016, Conference Track Proceedings*.
- [21] Alexander A. Sherstov and Peter Stone. 2005. Improving Action Selection in MDPs via Knowledge Transfer. In *Proceedings, The Twentieth National Conference on Artificial Intelligence and the Seventeenth Innovative Applications of Artificial Intelligence Conference, July 9-13, 2005, Pittsburgh, Pennsylvania, USA*. 1024–1029.
- [22] Alexander L. Strehl and Michael L. Littman. 2005. A theoretical analysis of Model-Based Interval Estimation. In *Machine Learning, Proceedings of the Twenty-Second International Conference (ICML 2005), Bonn, Germany, August 7-11, 2005*. 856–863.
- [23] Matthew E. Taylor and Peter Stone. 2009. Transfer Learning for Reinforcement Learning Domains: A Survey. *J. Mach. Learn. Res.* 10 (2009), 1633–1685.
- [24] Yee Why Teh, Victor Bapst, Wojciech M. Czarnecki, John Quan, James Kirkpatrick, Raia Hadsell, Nicolas Heess, and Razvan Pascanu. 2017. Distral: Robust multitask reinforcement learning. In *Advances in Neural Information Processing Systems 30: Annual Conference on Neural Information Processing Systems 2017, 4-9 December 2017, Long Beach, CA, USA*. 4496–4506.
- [25] Hado van Hasselt, Arthur Guez, and David Silver. 2016. Deep Reinforcement Learning with Double Q-Learning. In *Proceedings of the Thirtieth AAAI Conference on Artificial Intelligence, February 12-17, 2016, Phoenix, Arizona, USA*. 2094–2100.
- [26] Dian Wang, Colin Kohler, and Robert Platt. 2020. Policy learning in SE(3) action spaces. [arXiv:2010.02798 \[cs.RO\]](https://arxiv.org/abs/2010.02798)
- [27] Ziyu Wang, Tom Schaul, Matteo Hessel, Hado van Hasselt, Marc Lanctot, and Nando de Freitas. 2016. Dueling Network Architectures for Deep Reinforcement Learning. In *Proceedings of the 33rd International Conference on Machine Learning, ICML 2016, New York City, NY, USA, June 19-24, 2016*. 1995–2003.
- [28] Manuel Watter, Jost Tobias Springenberg, Joschka Boedecker, and Martin A. Riedmiller. 2015. Embed to Control: A Locally Linear Latent Dynamics Model for Control from Raw Images. In *Advances in Neural Information Processing Systems 28: Annual Conference on Neural Information Processing Systems 2015, December 7-12, 2015, Montreal, Quebec, Canada*. 2746–2754.
- [29] Tianhe Yu, Deirdre Quillen, Zhanpeng He, Ryan Julian, Karol Hausman, Chelsea Finn, and Sergey Levine. 2019. Meta-World: A Benchmark and Evaluation for Multi-Task and Meta Reinforcement Learning. In *3rd Annual Conference on Robot Learning, CoRL 2019, Osaka, Japan, October 30 - November 1, 2019, Proceedings*. 1094–1100.
- [30] Kevin Zakka, Andy Zeng, Johnny Lee, and Shuran Song. 2020. Form2Fit: Learning Shape Priors for Generalizable Assembly from Disassembly. In *2020 IEEE International Conference on Robotics and Automation, ICRA 2020, Paris, France, May 31 - August 31, 2020*. 9404–9410.
- [31] Andy Zeng, Shuran Song, Stefan Welker, Johnny Lee, Alberto Rodriguez, and Thomas A. Funkhouser. 2018. Learning Synergies Between Pushing and Grasping with Self-Supervised Deep Reinforcement Learning. In *2018 IEEE/RSJ International Conference on Intelligent Robots and Systems, IROS 2018, Madrid, Spain, October 1-5, 2018*. 4238–4245.
- [32] Andy Zeng, Shuran Song, Kuan-Ting Yu, Elliott Donlon, Francois Robert Hogan, Maria Bauzá, Daolin Ma, Orion Taylor, Melody Liu, Eudald Romo, Nima Fazeli, Ferran Alet, Nikhil Chavan Dafla, Rachel Holladay, Isabella Morona, Prem Qu Nair, Druck Green, Ian J. Taylor, Weber Liu, Thomas A. Funkhouser, and Alberto Rodriguez. 2018. Robotic Pick-and-Place of Novel Objects in Clutter with Multi-Affordance Grasping and Cross-Domain Image Matching. In *2018 IEEE International Conference on Robotics and Automation, ICRA 2018, Brisbane, Australia, May 21-25, 2018*. 1–8.

A STACKING GRAMMAR

Instead of arbitrarily choosing tasks, we characterize the whole family of possible tasks. Here, we define a simple grammar of stacking tasks. It only captures the notion of a stack, so it cannot represent tasks such as two blocks in a row. The only notion of two blocks being near one another is if a long block or a long roof can be put on top of them.

We have the following terminals: one block (1b), two blocks next to each other (2b), one brick (1l), short roof (1r) and long roof (2r). The non-terminals are ground (G), wildcard (W), short (S) and long (L). The starting symbol is the ground.

The rules allow for stacking of long objects (two blocks next to each other or one long block) on long objects, short on short and short on long. We separate the different possible outcomes of a rule by commas.

- $G \rightarrow 1bS, 2bW, 1lW$
- $W \rightarrow S, L$
- $S \rightarrow 1bS, 1b, 1r$
- $L \rightarrow 1lW, 2bW, 1l, 2b, 2r$

If we restrict the maximum height to three and only select structures that end with a roof, we get the 16 tasks used in our experiments.

B EXPERIMENT DETAILS

B.1 Fruits World

We use the same neural network for both the DQN and the action prior: it has two hidden layers with 256 neurons and we use the ReLU non-linearity in-between. The DQN predicts a Q-value for each action and the action prior predicts the log probability of an action being optimal for each action separately.

In the combination tasks, we train the initial policies from scratch. The DQNs are trained for 100k steps with an ϵ -greedy policy that linearly decreases from 1.0 to 0.1 over 80k steps. The learning rate was set to $5 * 10^{-4}$ and we use prioritized replay with default parameters, dueling network and double Q-learning [20, 25, 27].

Each action prior network is trained for 10k steps with a learning rate of 0.01. For the transfer experiments, we train a DQN with the same parameters as in the initial tasks, except it uses an action prior for exploration. During an exploration step, it samples an action proposed by the action prior ($\sigma = 0.5$); otherwise, it selects a random action.

In the sequence tasks, we first pre-train the DQNs for the initial tasks with expert demonstrations. We use a hand-crafted expert policy that select the optimal action with 0.5 probability and a random action otherwise. Then, we run 50k DQN training steps on this buffer and another 50k training steps, and then it is trained in the same way as the combinations DQN.

B.2 Simulated Block Stacking

We use a modified version of the U-Net architecture [17] for all our networks in this experiment. The schema of the fully-convolutional network is included in Figure 6.

To train the SDQfD, we collect 50k expert trajectories obtained by reversing deconstruction experience [30]. We pre-train model on this experience for 10k steps. Then we train the model while it interacts with the simulator for 40k episode. Each episode has a maximum length

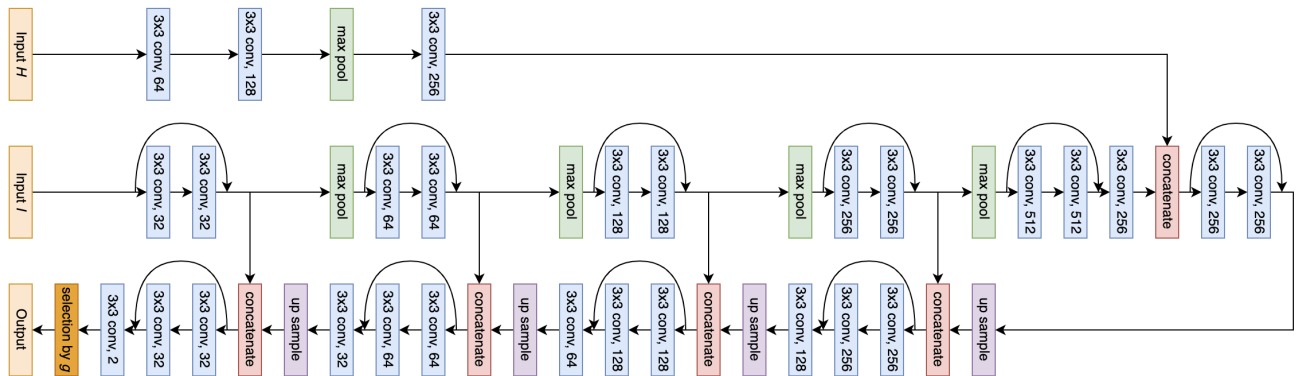


Figure 6: A modified U-Net network architecture. The inputs are a 90×90 depth image of the environment I and a 24×24 zoomed-in image of an object the robot picked up. If the robot is not holding anything, all pixel values are set to zero. 3×3 conv, 32 means a convolutional layer with 32 filters of size 3. All max pooling layers use a kernel of size 2 and a stride of 2. We omit the ReLU activations in the diagram.

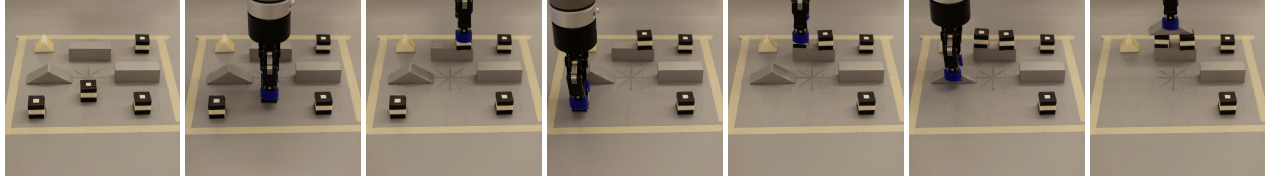


Figure 7: One example run of the 1l2b2r task.

of 20. The learning rate is set to $5 * 10^{-5}$ and both the large margin weight and the margin coefficients are set to 0.1. There is no exploration, the batch size is set to 32 and the discount to 0.9. We run five simulated environments in parallel—we take one step in each environment, collect the transitions, take one training step of the SDQfD and repeat.

For the training datasets, we collect 20k steps for each of the 15 tasks used to train an action prior and concatenate the experience. The task classifier is trained on this data for 20k steps with a learning rate of 10^{-3} , weight decay of 10^{-5} and batch size set to 32. We use a probability threshold for relevant tasks θ of 0.05. Action priors are trained with the same settings except for a batch size of 50 for 10k training steps.

In the transfer experiment, we use an action prior probability threshold σ of 0.1. During exploration, the model only selects actions proposed by the action prior. We train a DQN for 100k episodes with the modified ϵ -greedy policy. ϵ linearly decays from 1.0 to 0.01 for 80k episodes. The learning rate is set to 10^{-4} , batch size to 32 and the discount factor to 0.9. We use prioritized experience replay with default parameters, but we do not use the weighting of the sampled transitions in the loss function.

In the weight sharing experiments, the weights L^2 penalty ω_{WS} is set to 0.1.

B.3 Real-World Block Stacking

We tested the trained model on a Universal Robots UR5 arm with a Robotiq 2F-85 Gripper. The observation is provided by an Occipital Structure sensor pointing to the workspace from top-down. Figure 5 shows the robot experiment setup. All task parameters mirror the simulation. We run 10 trials for each task, and the maximum number of steps for each trial is 20. Figure 7 shows an example run of task 1l2b2r.

C ADDITIONAL RESULTS

Table 8 shows results for experiment #2 (Section 6.3) for all 16 tasks. As we stated in the main text, we found that task classifier helps in complex tasks and decreasing the probability threshold σ tends to increase the success rates of the action priors that use the task classifier.

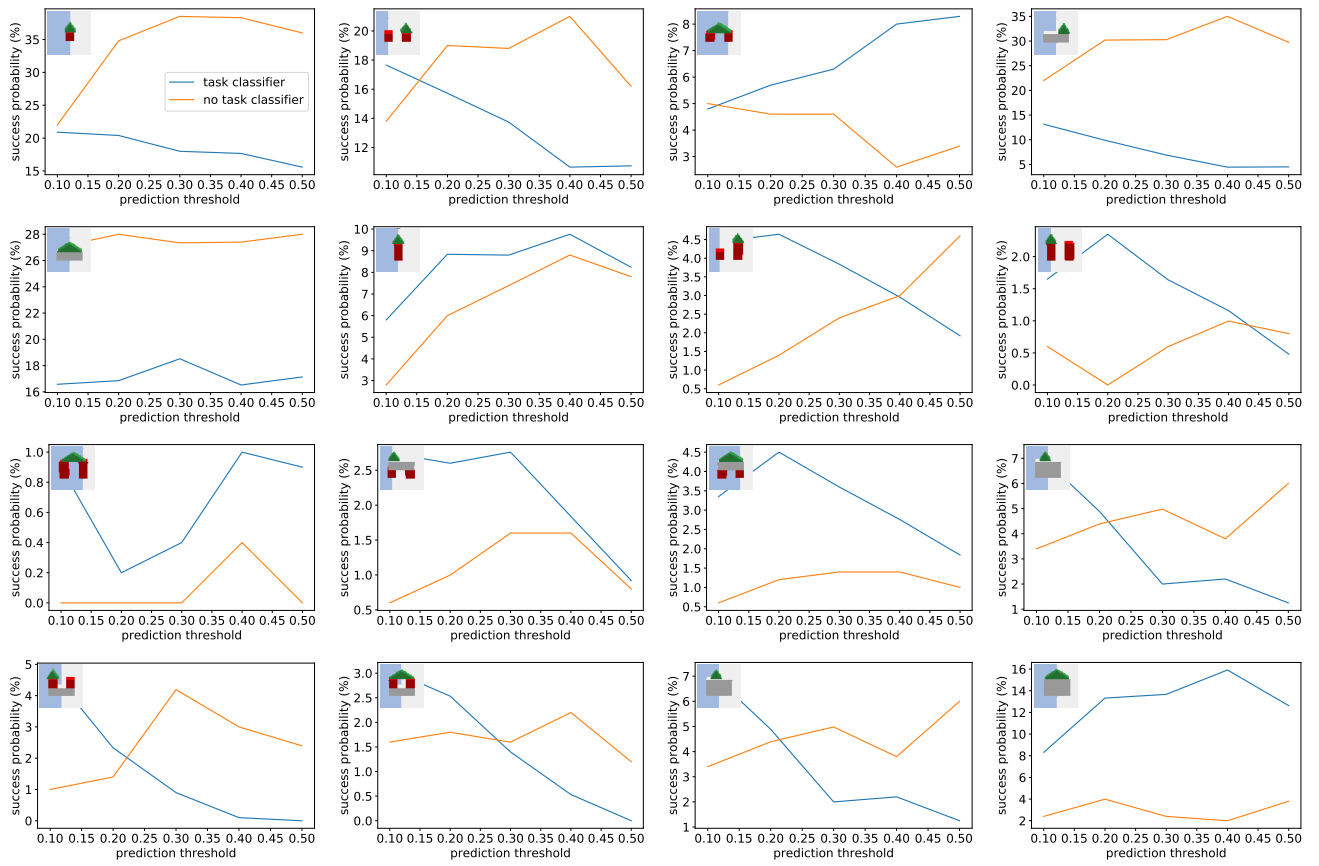


Figure 8: We show the same results as in Figure 4 in the main test, but for all 16 tasks